Tetrahedron 69 (2013) 9544–9550

Contents lists available at ScienceDirect

Tetrahedron

journal homepage: www.elsevier.com/locate/tet

The preparation and properties of bulk-heterojunction organic solar cells with indole-containing fulleropyrrolidine derivatives as acceptors

Xiaona Zhang [a,b,†], Liang Sun [a,c,†], Wei Zheng [b], Xichang Bao [a], Ning Wang [a,*], Ting Wang [a], Renqiang Yang [a,*]

[a] Qingdao Institute of Bioenergy and Bioprocess Technology, Chinese Academy of Sciences, Qingdao 266101, China
[b] College of Materials Science and Engineering, Harbin University of Science and Technology, Harbin 150080, China
[c] University of Chinese Academy of Sciences, Beijing 100049, China

ARTICLE INFO

Article history:
Received 27 June 2013
Received in revised form 13 September 2013
Accepted 16 September 2013
Available online 21 September 2013

Keywords:
Photovoltaic effect
Fullerene derivative
Indole
Electron acceptor

ABSTRACT

Two indole-containing fullerene derivatives, *N*-hydrogen-2-[3-(*N*-2-ethylhexylindolyl)][60]fulleropyrrolidine (EHIHC60P), and *N*-(2-ethylhexylindolyl))-2-[3-(*N*-2-ethylhexylindolyl)][60]fulleropyrrolidine (DEHIC60P) were synthesized by the typical Prato reaction. The absorption spectra, electrochemical properties of the two compounds were measured. Inverted solar cells were fabricated with the structure of ITO/ZnO/poly(3-hexylthiophene) (P3HT):fullerene derivatives/MoO_3/Ag. The highest power conversion efficiencies (PCEs) of 3.32% and 3.23% were obtained for P3HT/EHIHC60P and P3HT/DEHIC60P based solar cells at the composite ratio of 1:1 after the active layers were annealed at 150 °C under inert atmosphere, with a open-circuit voltage (V_{oc}) of 0.66 V and 0.74 V, respectively. For comparison, the device based on P3HT/PCBM at the same conditions showed the PCE of 3.28%, with a V_{oc} of 0.61 V. The influence on the photovoltaic property of the fullerene derivatives, which was induced by some subtle changes in the chemical structure was compared and discussed.

1. Introduction

Organic photovoltaic devices (OPVs) have been widely regarded as one of the candidates to solve the energy crisis, and attract an extensive attention due to their light weight, low cost, and flexible features.[1–4] Since the introduction of bulk-heterojunction (BHJ) concept in 1995,[5] organic solar cells with the BHJ active layer, which consists of conjugated polymer as donor and fullerene derivative as acceptor, have been extensively studied.[6–10] Recently, the power conversion efficiency (PCE) of OPVs has exceeded 10%.[11] The donor–acceptor (D–A) type conjugated copolymers, which have broad range of light absorption, significantly enhance the light-harvesting ability of the active layers in the photovoltaic devices.[12] In the past decades, considerable efforts have been made on the design and preparation of novel D–A type conjugated donor materials. The innovation on the structure of D–A conjugated copolymers has become the main driving force to improve the efficiency of the photovoltaic device.[13] In contrast, researches on the structure–property relationship of the acceptor materials are limited. Until now, the most widely used acceptor material is still phenyl-C61-butyric acid methyl ester (PCBM),[14,15] which offers good solubility in organic solvents, but also suffers from the drawbacks such as weak absorption in the visible region, relatively low lowest unoccupied molecular orbital (LUMO) energy, and large scale aggregation.[16,17] Recently, more attentions have been paid on the development of new fullerene derivatives other than PCBM to further improve the performance of OPVs through the pathway of the acceptor materials.[18–23] For instance, Li et al. reported a remarkable indene substituted fullerene bisadduct (ICBA).[24] OPVs based on poly(3-hexylthiophene) (P3HT)/ICBA showed PCE of 5.44% with V_{oc} of 0.84 V, and the PCE can be up to 6.5% after further device optimization.[25] Matsuo and co-workers reported OPVs with silylmethylfullerene (SIMEF) as acceptor, which showed higher PCE than that using PCBM.[26] Lately, a 54π-electron fullerene acceptor, called bis-TOQMF, has been developed and given the PCE of 4.56% when applied in OPVs by Ding et al.[27] Other fullerene derivatives, such as indolinone-substituted methanofullerene,[28] thieno-*o*-quinodimethane fullerene multi-adducts,[29] diarylmethanofullerene,[30] dibenzosuberane-substituted fullerene derivatives,[31] 2-benzyl-1,2-dihydro[60]fullerenes,[18] methanofullerene derivative,[32] and alkoxy-substituted dihydronaphthyl-based [60]fullerene bisadduct derivatives,[33] were prepared and used as acceptors in the active

* Corresponding authors. Tel.: +86 532 80662700; fax: +86 532 80662778; e-mail addresses: wangning@qibebt.ac.cn (N. Wang), yangrq@qibebt.ac.cn (R. Yang).
† X.Z. and L.S. contributed equally to this work.

0040-4020/$ – see front matter © 2013 Elsevier Ltd. All rights reserved.
http://dx.doi.org/10.1016/j.tet.2013.09.046

layer of the photovoltaic devices. All the above reports indicated that new fullerene derivatives with proper energy levels, mobility, and compatibility also play a pivotal role in improving the performance of OPVs, and the photovoltaic properties of the fullerene derivatives could be tuned and optimized by altering the substitute groups on the fullerene derivatives.[19,34]

Herein, two fulleropyrrolidine derivatives EHIHC60P and DEHIC60P were designed and prepared (the structures were shown in Scheme 1). In the case of EHIHC60P, 3-(*N*-2-ethylhexylindolyl) group was connected to the pyrrolidine ring. The indole-containing substitute group was selected due to its excellent electron-donating property.[23,28] To further improve the photovoltaic performance of the indole-containing fulleropyrrolidine derivatives, the second indole-containing substituted group ((1-(2-ethylhexyl)-1*H*-indol-3-yl)methyl group) was introduced to the N atom of the pyrrolidine ring, thus the LUMO level of the fullerene derivative DEHIC60P (Scheme 1) could be further raised in some extent, which would result in higher V_{oc} values of photovoltaic devices.[12] Compared to the previously reports of the multi-adduct fullerene derivatives, our strategy has the advantage of avoiding the isomers and energy disorder while controllable enhancing the LUMO level of the acceptors.[14,15,24,29–33] Meanwhile, ethylhexyl alkyl chain on nitrogen atom in the indole ring could improve the solubility of fulleropyrrolidine derivatives and miscibility with the donor polymers.[35] The structure–property relationship of fullerene derivatives was investigated. The influence on the photovoltaic property, which was induced by some subtle changes in the chemical structure such as the amount and connection mode of the electron-donating groups, was carefully compared and discussed.

about 430 nm and a weak peak at about 700 nm, which is consistent with the literature.[37] These results clearly indicate that the absorption characteristics of the functionalized fullerene derivatives are governed by the π system of the fullerene. It is obvious that the absorption intensity of EHIHC60P and DEHIC60P is much stronger than that of PCBM at the same concentration, which could be due to the contribution of the indole functional groups. Meanwhile, DEHIC60P shows stronger absorption than EHIHC60P, which is expected to be beneficial to their application in OPVs. As shown in Table 1, the optical bandgaps estimated from the absorption edges of EHIHC60P and DEHIC60P are both 1.71 eV, which are almost same as that of PCBM (1.73 eV). The energy bandgaps did not show obvious change when the indole substitute groups were conjugation-interruptedly linked on fulleropyrrolidine ring.

2.3. Electrochemical properties

Electronic energy levels (especially the LUMO levels) of the fullerene derivatives are crucial for their application in OPVs as acceptors. To evaluate the redox behaviors of the synthesized fullerene derivatives, the electrochemical properties of EHIHC60P, DEHIC60P, and PCBM were measured by cyclic voltammetry (CV) in *o*-dichlorobenzene with 0.04 M Bu_4NPF_6 as the supporting electrolyte. Both fullerene derivatives exhibited three quasi-reversible reduction waves in the negative potential range from 0 to −2.5 V (vs Ag/AgCl) as shown in Fig. 2. The onset reduction potentials (E_{red}^{onset}) of EHIHC60P and DEHIC60P were slightly shifted to negative region, indicating higher LUMO en-

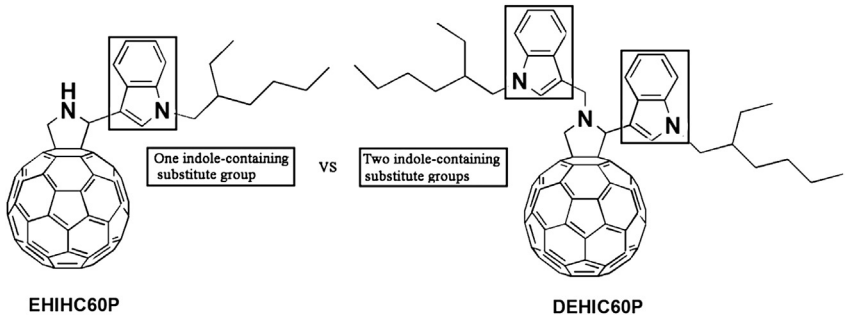

Scheme 1. The design strategy and the structures of fulleropyrrolidine derivatives with one (EHIHC60P) or two (DEHIC60P) indole substitute groups.

2. Results and discussion

2.1. Synthesis

Indole-containing fullerene derivatives EHIHC60P and DEHIC60P were synthesized conveniently via a 1,3-dipolar cycloaddition reaction[36] (as shown in Scheme 2). The reaction time was optimized to avoid the multi-addition adducts, which could lead to a relative low yield of the target compound. EHIHC60P and DEHIC60P have good solubility in the common organic solvents such as chloroform, toluene, chlorobenzene, and *o*-dichlorobenzene. They are readily purified by column chromatography to give the target product in high purity.

2.2. Optical properties

Fig. 1 shows the ultraviolet–visible (UV–vis) absorption spectra of EHIHC60P and DEHIC60P in chloroform (10^{-5} mol/L). The absorption band in the region of 300–800 nm is similar for each derivative. As shown in the inset of Fig. 1, there is a sharp peak at

ergy levels than that of PCBM. It could be attributed to the electron-donating effect from the substituted indole groups on the fullerene ring, which raise the LUMO energy level. The LUMO energy levels of the fullerene derivatives were estimated from their onset reduction potentials according to the equation $LUMO = -[(E_{red}^{onset} - E_{fc}) + E_{ref}]$ (eV), where E_{Fc} is the potential of the external standard, the ferrocene/ferrocenium ion (Fc/Fc^{+}) couple, and E_{ref} is the reference energy level of ferrocene (4.8 eV below the vacuum level; the vacuum level is defined as zero). The experimental values of EHIHC60P, DEHIC60P, and PCBM are summarized in Table 1, which also contains the theoretical energy levels calculated from the density functional theory (DFT) for comparison. As shown in Table 1, the LUMO energy levels of EHIHC60P and DEHIC60P are −3.65 and −3.60 eV, which are raised by 0.08 and 0.13 eV in comparison with that of PCBM (−3.73 eV), respectively. The experimental LUMO levels of the acceptors were in reasonable agreement with the calculated results. The higher LUMO energy levels are desirable for higher open-circuit voltages of OPVs. Frontier molecular orbital (HOMO and LUMO) for the acceptors is shown in Table S1.

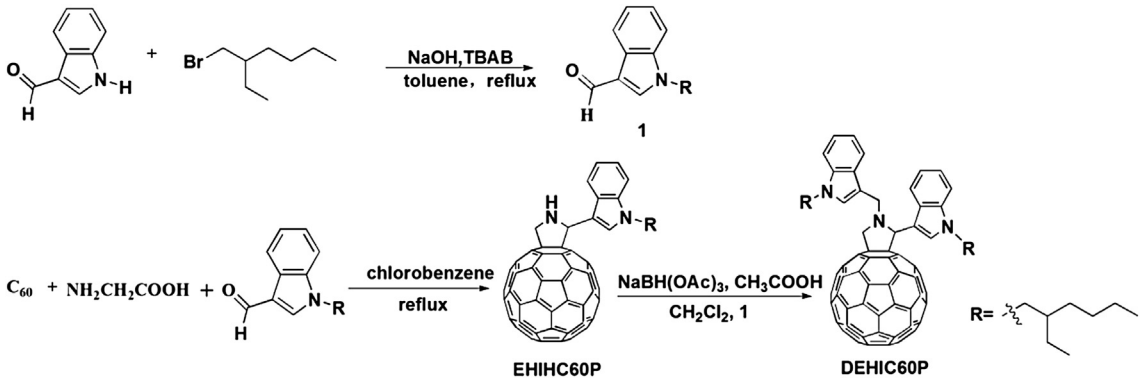

Scheme 2. Synthetic routes of EHIHC60P and DEHIC60P.

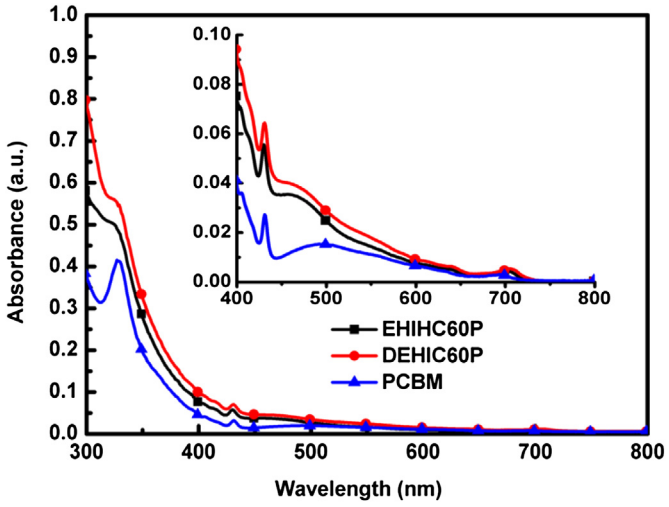

Fig. 1. UV–visible absorption spectra of EHIHC60P, DEHIC60P, and PCBM in chloroform solution (10^{-5} mol/L).

2.4. Photovoltaic performance

In order to investigate the potential application of the two fullerene derivatives in solar cells, EHIHC60P and DEHIC60P were used as acceptors to fabricate inverted photovoltaic devices with commercial P3HT as donor. Different weight ratios, 1:1.2, 1:1, 1:0.8, and 1:0.6 of the donor to acceptor were varied to optimize the composition of the blend film. Each device was prepared under the same conditions (annealed at 150 °C for 10 min). Fig. 3 shows the current density–voltage (J–V) curves of the devices under the illumination of AM1.5G 100 mW/cm^2, and the detailed device parameters are summarized in Table 2. It can be observed that the device using P3HT/EHIHC60P as the active layer showed similar open-circuit voltages regardless of the composite ratio but exhibited different short-circuit currents and fill factors (FF). The results indicated that the ratio of 1:1 showed the highest efficiency of 3.32%, with V_{oc}=0.66 V, J_{sc}=8.4 mA/cm^2, and FF=59.9%. As shown in Fig. 3b, the highest PCE of 3.23% for the P3HT/DEHIC60P based device was obtained at the 1:1 composite ratio with V_{oc}=0.74 V, J_{sc}=7.09 mA/cm^2, and FF=61.3%. For comparison, the device based on P3HT/PCBM in a weight ratio of 1:1 was made as a reference exhibiting the PCE of 3.28%. The measured V_{oc} values of EHIHC60P and DEHIC60 are higher than that of the device using PCBM as acceptor (Table 2). In general, the open-circuit voltage (V_{oc}) is proportional to the difference between the HOMO energy level of donor and the LUMO energy level of fullerene derivatives.[38] The results are consistent with the LUMO levels of the EHIHC60P and DEHIC60P, which are 0.08 and 0.13 eV higher than that of PCBM, respectively. It should be noted that the DEHIC60P, which has two functional indole groups, exhibits a higher V_{oc} value than that of EHIHC60P due to the additional electron-donating effect of the indole substituted groups on pyrillidine ring, however, their J_{sc} values are inverse. It could be attributed to the existence of two ethylhexyl alkyl chains in DEHIC60P, which increases steric hindrance between the compounds and thus affects the efficient charge carrier transportation in the active layer.[39]

In order to investigate the effect of processing additive on the performance of devices, P3HT/fullerene derivatives blend films were prepared from solution in chlorobenzene with addition of 1 wt %, 2.5 wt %, and 4 wt % 1-chloronaphthalene (CN) as

Table 1
Energy levels obtained from experiments and theoretical calculations

	Experimental values[a]			Theoretical values[b]		
	HOMO (V)	LUMO (eV)	Eg^{opt} (eV)	HOMO (eV)	LUMO (eV)	Eg (eV)
EHIHC60P	−5.36	−3.65	1.71	−5.66	−3.25	2.40
DEHIC60P	−5.31	−3.60	1.71	−5.46	−3.20	2.26
PCBM	−5.46	−3.73	1.73	−5.88	−3.36	2.53

[a] LUMO values were determined by CV results, while HOMO values were estimated by subtracting from optical gap (Eg^{opt}).
[b] All chemical structures were optimized with the B3LYP function and DEF2-SVP.

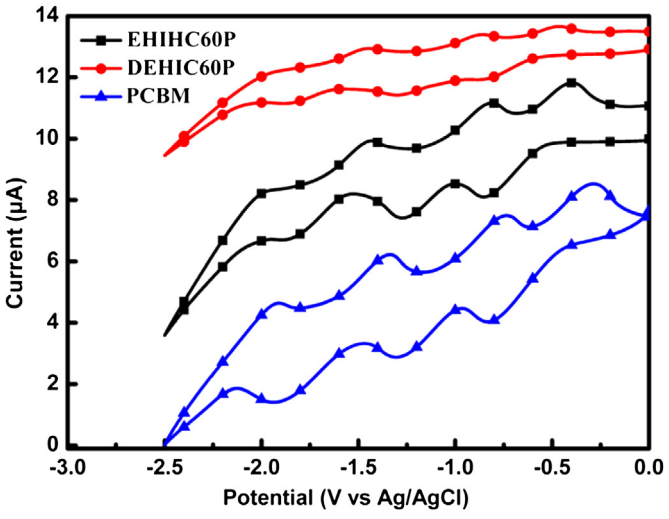

Fig. 2. Cyclic voltammograms of EHIHC60P, DEHIC60P, and PCBM.

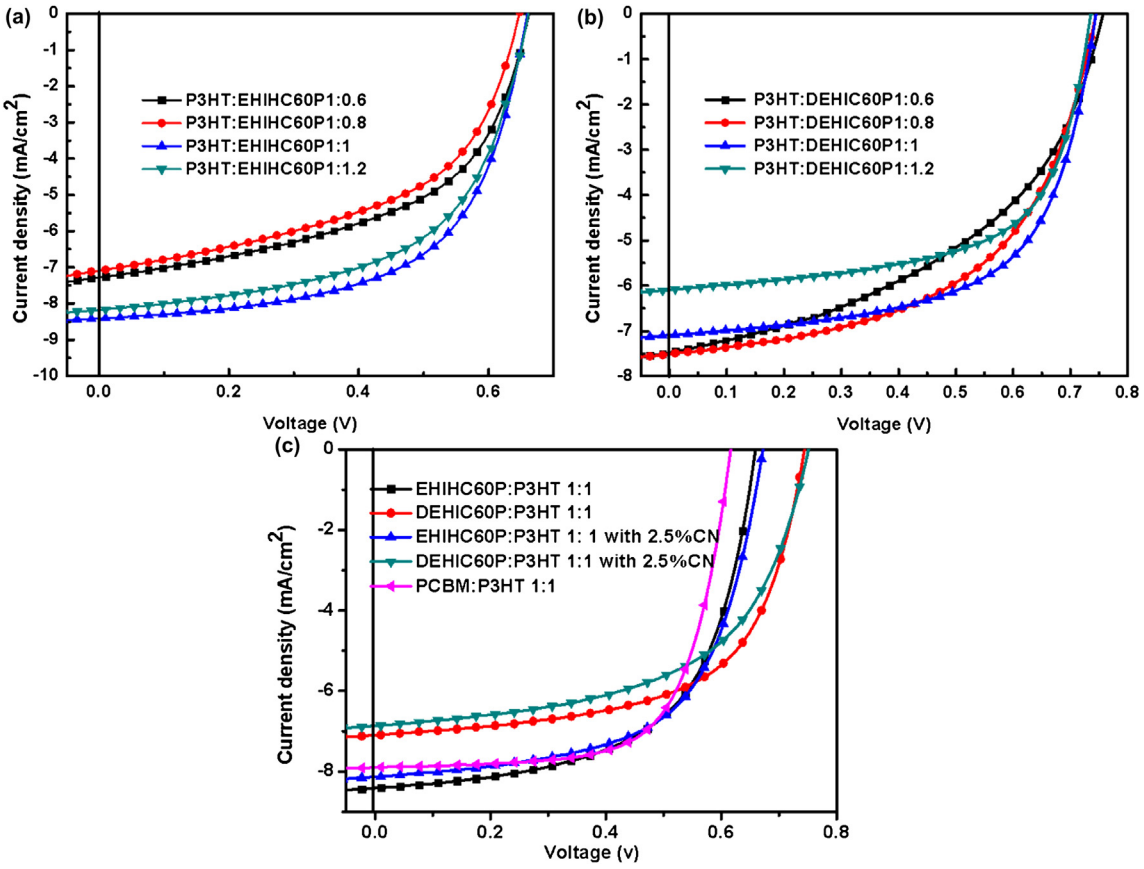

Fig. 3. *J*–*V* curves of the devices fabricated using (a) P3HT:EHIHC60P and (b) P3HT:DEHIC60P as active layers with different weight ratios under AM1.5G illumination (100 mW/cm^2); (c) P3HT/fullerenes=1:1 with and without 2.5% CN, and annealed P3HT/PCBM=1:1 blend films.

a cosolvent, respectively. CN has a high boiling point (250 °C), and adding CN as additive has been proved to be a particularly effective way to tune the phase separation of the active layer.[40–42] Fig. 3c shows the effect of additives on the polymer solar cell performance and the results are summarized in Table 3. It can be seen that both the fullerene derivatives show the highest efficiency when mixing 2.5% CN to the solvent. However, no significant changes on the performance are observed compared to the annealing treatment. The introduction of CN leads to a small increase in FF from 59.9% to 61.1% for the P3HT/EHIHC60P system, and a decrease from 61.3% to 56.6% for P3HT/DEHIC60P. The V_{oc} values are nearly invariable with and without CN additives for the two derivatives. On the contrary, J_{sc} decreases from 8.40 to 8.12 mA/cm^2 for the P3HT/EHIHC60P, and from 7.09 to 6.85 mA/cm^2 in the case of P3HT/DEHIC60P. Consequently, the PCE remains unchanged for the P3HT/EHIHC60P system, and decreases from 3.23% to 2.91% for the P3HT/DEHIC60P. The above results indicated the different effect of adding CN additives on the devices with EHIHC60P or DEHIC60P as acceptors. We attribute this to the difference of chemical structure of the two fullerene derivatives, which obviously varies the properties of the acceptors, such as the solubility and the miscibility with the donor polymer.[43–45]

Table 2
Device performance of the active layers without additives

Active layers	Ratio	Solvent	J_{sc} (mA/cm^2)	V_{oc} (V)	FF (%)	PCE (%)
P3HT/EHIHC60P	1:0.6	CB	7.27	0.67	52.6	2.53
	1:0.8	CB	7.08	0.66	51.4	2.35
	1:1.0	CB	8.40	0.66	59.9	3.32
	1:1.2	CB	8.17	0.66	57.2	3.09
P3HT/DEHIC60P	1:0.6	CB	7.45	0.76	46.1	2.60
	1:0.8	CB	7.50	0.74	54.0	3.01
	1:1.0	CB	7.09	0.74	61.3	3.23
	1:1.2	CB	6.09	0.73	62.6	2.80
P3HT/PCBM	1:1.0	CB	7.89	0.61	67.6	3.28

Table 3
Device performance of the active layers with CN additive treatment

Active layers	Additive	J_{sc} (mA/cm^2)	V_{oc} (V)	FF (%)	PCE (%)
P3HT/EHIHC60P (1:1)	CN 1%	7.23	0.69	51.6	2.56
	CN 2.5%	8.12	0.67	61.1	3.33
	CN 4%	8.00	0.68	59.8	3.27
P3HT/DEHIC60P (1:1)	CN 1%	2.62	0.78	31.5	0.64
	CN 2.5%	6.85	0.75	56.6	2.91
	CN 4%	7.00	0.73	50.6	2.58

The external quantum efficiencies (EQEs) were measured with the optimized device conditions for P3HT/fullerene derivatives with or without CN additive. A relatively broad photo response range from 320 nm to 650 nm can be seen in Fig. 4, and the spectra between 450 and 650 nm are mainly due to the P3HT absorbance (see Fig. S1). The optimized devices based on P3HT/EHIHC60P, P3HT/EHIHC60P with 2.5% CN, P3HT/DEHIC60P and P3HT/DEHIC60P with 2.5% CN show maximum EQEs values of 51.4%, 48.8%, 46.3%, and 41.1% at 515 nm, respectively. EHIHC60P shows slightly higher EQE value than that of DEHIC60P, which is coincident with the measured J_{sc} values in the photovoltaic devices.

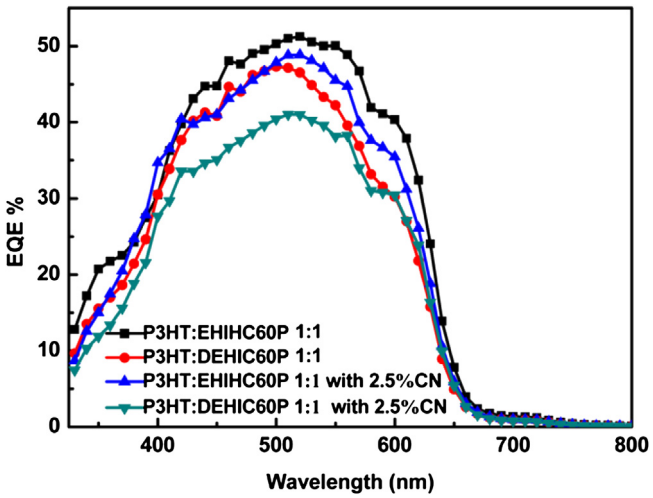

Fig. 4. External quantum efficiency (EQE) curves of P3HT/EHIHC60P and DEHIC60P with or without additive, respectively.

2.5. Morphology analysis

The morphologies of the blend films of P3HT and fullerene derivatives have been investigated by tapping-mode atomic force microscopy (AFM). Figs. 5 and 6 show the topographic and phase images of the films after annealing or adding CN additive treatment, respectively. All the films were prepared under the same conditions with the optimized photovoltaic devices. As shown in Figs. 5a and 6a, the surface root mean square (rms) roughness for the blend film of P3HT/DEHIC60P after annealing treatment is 1.13 nm, which is 0.1 nm smaller than that of the P3HT/EHIHC60P. The result indicates that the (1-(2-ethylhexyl)-1*H*-indol-3-yl) methyl substituted group on the pyrrolidine ring of DEHIC60P tends to improve the miscibility with P3HT. As shown in Figs. 5b and 6b, when the blend films are spin-coated from chlorobenzene solution containing 2.5% CN as additive, the rms data of P3HT/EHIHC60P and P3HT/DEHIC60P are greatly increased to 5.51 and 3.82 nm, respectively, which indicates that adding CN as additive in the mixture leads to rougher surface than annealing treatment. Interestingly, the fibrous networks phase images are observed in the blending films with CN additives, indicating that a well-ordered phase separation between P3HT and EHIHC60P or DEHIC60P is formed (Figs. 5d and 6d). To investigate the crystallinity of the blend films with and without CN as additives, the X-ray diffraction (XRD) spectra of the blend films were measured. As shown in Fig. S2, the blend films with CN as additive showed higher P3HT diffraction peaks than those of only annealing films, which indicated that the films spin-coated from chlorobenzene solution containing CN as additive had higher crystallinity than those of annealed blend films.[23,46] However, the rougher surface morphology may induce poorer contact between the active layer and the cathode, which could partially offset the favorable phase separation and crystallinity of the blend films.[47,48]

3. Conclusions

Two new fullerene derivatives EHIHC60P and DEHIC60P were synthesized, and they showed much higher molar absorption coefficient than that of PCBM due to the contribution of the indole functional groups. The CV results indicated that the LUMO energy levels of EHIHC60 and DEHIC60P were 0.08 and 0.13 eV higher than that of the PCBM, respectively, which was due to the electron-donating effect of the indole substituted group. This work indicated that indole functional unit is an excellent electron-donating substituted group to modify the fullerene core, and thus their energy levels can be tuned when the indoles are

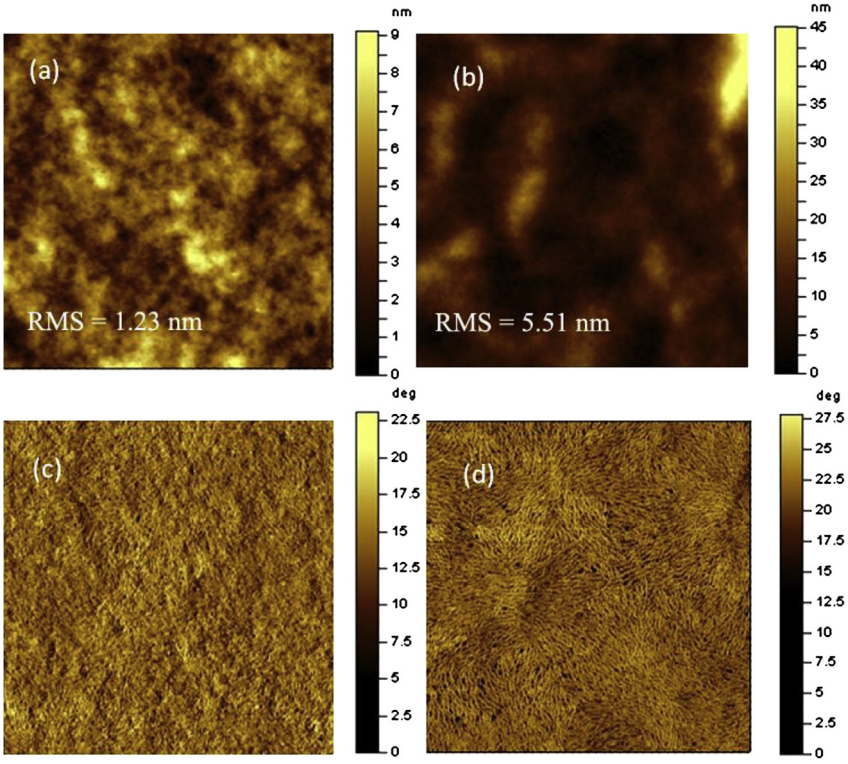

Fig. 5. The AFM tapping mode height (a) and phase (c) images (2 μm×2 μm) of the P3HT/EHIHC60P (1:1, w/w) film annealed at 150 °C for 10 min without additive, and height (b), phase (d) images (2 μm×2 μm) of the blend film with 2.5% CN additive.

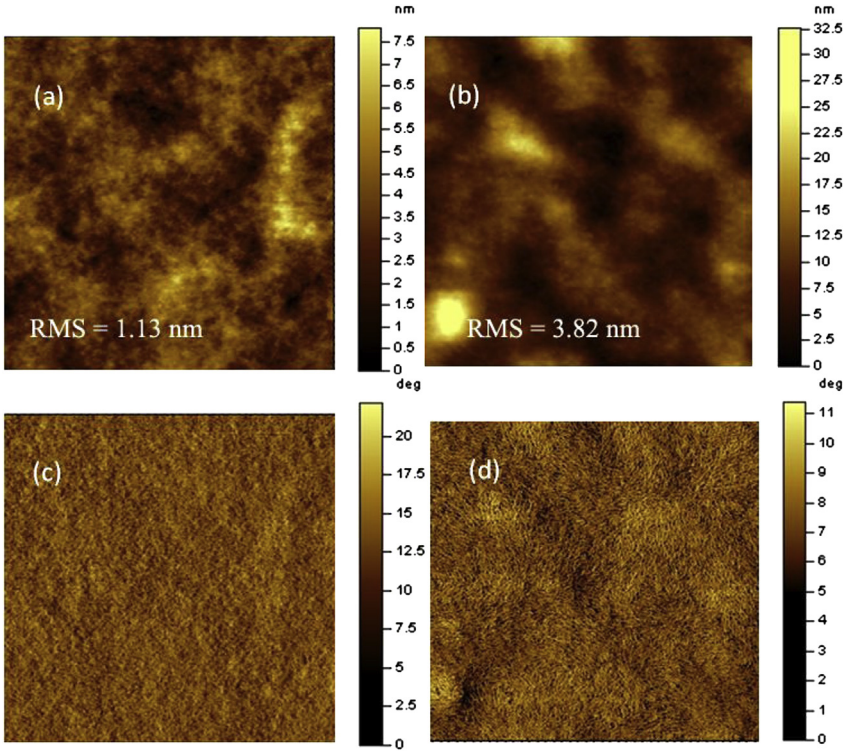

Fig. 6. The AFM tapping mode height (a) and phase (c) images (2 μm×2 μm) of the P3HT:DEHIC60P (1:1, w/w) film annealed at 150 °C for 10 min without additive, and height (b), phase (d) images (2 μm×2 μm) of the blend film with 2.5% CN additive.

substituted on the fullerene rings. The photovoltaic devices were fabricated with inverted structure of ITO/ZnO/P3HT:fullerene derivatives/MoO_3/Ag. The optimized blend ratio of donor to acceptor was found to be 1:1 for both of the two fullerene derivatives, and the highest PCEs of the devices using EHIHC60P and DEHIC60P were 3.32% and 3.23%, respectively, after the active layers were annealed at 150 °C under inert atmosphere. Interestingly, the fullerene derivatives EHIHC60P and DEHIC60P showed higher V_{oc} values than that of PCBM, which were consistent well with their different LUMO levels. It should be noted that the fulleropyrrolidine derivatives EHIHC60P and DEHIC60P showed substantially equivalent PCEs to that of the PCBM, indicating they are promising acceptors for the bulk-heterojunction organic solar cells. Subsequently, CN was used as processing cosolvent additive, which had significant effect on the morphology of the active layer and obtained well-ordered nano-fibrous phase separation. However, no obvious changes on the photovoltaic performance were observed, which was probably due to the enhancement surface roughness of the active layer and thus the charge collection decreased. More efforts to develop highly efficient acceptors based on indole-containing fulleropyrrolidine derivatives are currently on going in our group.

4. Experimental

4.1. Materials

C_{60} was purchased from Henan Puyang Fullerene Technology Co., Ltd. Indole-3-carboxaldehyde, 2-ethylhexyl bromide, tetrabutylammonium bromide, and glycine were obtained from Aladdin Reagent Corporation. P3HT was purchased from Lumtec Inc. Solvents such as toluene, chlorobenzene, dichloromethane, and acetic acid were commercially obtained and purified with standard methods.

4.2. Measurements

^{1}H NMR and ^{13}C NMR spectra were recorded using a Bruker DRX-600 spectrometer. The APCI-TOF HRMS were performed on Bruker Maxis UHR-TOF (both positive and negative ion reflector mode). The UV–vis spectra were measured on a Varian Cary 50 spectrophotometer. CV measurement was performed on a CHI660D electrochemical workstation, and it was measured in anhydrous *o*-dichlorobenzene containing 0.04 M tetra(*n*-butyl)ammonium hexafluorophosphate (Bu_4NPF_6) as the supporting electrolyte at a scan rate of 100 mV/s under argon atmosphere. Glassy carbon, platinum wire, and Ag/AgCl were used as working, counter, and reference electrodes, respectively. The potential of ferrocene/ferrocenium (Fc/Fc^+) was measured to be 0.6 V compared to the Ag/AgCl electrode under the same conditions. It is assumed that the redox potential of Fc/Fc^+ has an absolute energy level of −4.8 eV to vacuum.[49] AFM images were acquired with an Agilent 5400 scanning probe microscope with a Nanodrive controller in tapping mode. The crystallization of the active layer was analyzed using XRD (Mac Science, Cu Kα wavelength of 0.154056 nm). The blend films of P3HT and fullerene derivatives for AFM and XRD were prepared under the same experimental conditions as that of optimized photovoltaic devices fabrication. DFT calculations were performed using the Gaussian 09 package with the nonlocal hybrid Becke three-parameter Lee–Yang–Parr (B3LYP) function and the 6-31G* basis set to obtain the HOMO and LUMO levels after optimizing the geometry of materials using the same method. Within the ORCA program, the RI approximation was taken to speed up the calculations and thus the def2-SVP basis set was used.

4.3. Fabrication of photovoltaic devices

The inverted photovoltaic devices with the structure of ITO/ZnO/active layer/MoO_3/Ag were prepared under conditions as

follows. All cells were fabricated on ITO coated glass substrates with a nominal sheet resistance of 15 Ω/sq. The substrates were cleaned in an ultrasonic bath with detergent, ultra pure water, acetone, and isopropyl alcohol sequentially for 20 min, and then dried in a laboratory oven at 80 °C for one night. The ITO surfaces were coated by the sol–gel ZnO with spin-coated speed at 2000 rpm for 40 s, and then, treated in an oven for 16 h at 100 °C. The P3HT and our synthesized fullerene derivatives were dissolved in chlorobenzene (15 mg/mL) with or without 1-chloronaphthalene (CN) additive in different weight ratios of 1:1.2, 1:1, 1:0.8, and 1:0.6, respectively. After stirring for 4 h, the blend solution was then spin-coated on ZnO-coated ITO substrate to form the active layer at 2200 rpm with thickness of 70 nm. Followed by annealing at 150 °C for 10 min, a thin layer of MoO_3 (3 nm) and Ag (80 nm) was thermal evaporated with VPC-1100 under 2.0×10^{-5} Pa to complete the inverted structure. Finally, the cells with an active area of 0.1 cm^2 were measured. The fabrication process of the device was conducted in the nitrogen glovebox. The film thickness was measured with Veeco Dektak 150 surface profiler. The current density–voltage (J–V) characteristics were recorded with Keithley 2420 source measurement unit under simulated 100 mW/cm^2 (AM1.5G) irradiation from a Newport solar simulator. EQE of solar cells was analyzed by certified Newport incident photon conversion efficiency (IPCE) measurement system.

Acknowledgements

This work was supported by the Ministry of Science and Technology of China (2010DFA52310), National Natural Science Foundation of China (21204097, 51173199, 61107090), Chinese Academy of Sciences (KGCX2-YW-399+9-2), Department of Science and Technology of Shandong Province (2010GGC10345), Shandong Provincial Natural Science Foundation (ZR2011BZ007), Qingdao Municipal Science and Technology Program (11-2-4-22-hz), and the Key Project Foundation of Heilongjiang Province University Material Research and Application Key Laboratory (2013).

Supplementary data

DFT calculation structures of the acceptors, absorption spectra and XRD spectra of blend films, and detailed synthesis procedure and characterization of the compounds described in this article. Supplementary data associated with this article can be found in the online version, at http://dx.doi.org/10.1016/j.tet.2013.09.046.

References and notes

1. Kim, J. Y.; Lee, K.; Coates, N. E.; Moses, D.; Nguyen, T.-Q.; Dante, M.; Heeger, A. J. *Science* **2007**, *317*, 222–225.
2. Liu, H. B.; Xu, J. L.; Li, Y. J.; Li, Y. L. *Acc. Chem. Res.* **2010**, *43*, 1496–1508.
3. Li, H. M.; Li, Y. L.; Zhai, J.; Cui, G. L.; Liu, H. B.; Xiao, S. Q.; Liu, Y.; Lu, F. S.; Jiang, L.; Zhu, D. B. *Chem.—Eur. J.* **2003**, *9*, 6031–6038.
4. Moriwaki, K.; Matsumoto, F.; Takao, Y.; Shimizu, D.; Ohno, T. *Tetrahedron* **2010**, *66*, 7316–7321.
5. Yu, G.; Gao, J.; Hummelen, J. C.; Wudl, F.; Heeger, A. J. *Science* **1995**, *270*, 1789–1791.
6. He, Y.; Li, Y. *Phys. Chem. Chem. Phys.* **2011**, *13*, 1970–1983.
7. Li, C.-Z.; Yip, H.-L.; Jen, A. K. Y. *J. Mater. Chem.* **2012**, *22*, 4161–4177.
8. Dou, L.; Chang, W. H.; Gao, J.; Chen, C. C.; You, J.; Yang, Y. *Adv. Mater.* **2013**, *25*, 825–831.
9. He, Z.; Zhong, C.; Huang, X.; Wong, W. Y.; Wu, H.; Chen, L.; Su, S.; Cao, Y. *Adv. Mater.* **2011**, *23*, 4636–4643.
10. Wang, N.; Li, Y. J.; He, X. R.; Gan, H. Y.; Li, Y. L.; Huang, C. S.; Xu, X. H.; Xiao, J. C.; Wang, S.; Liu, H. B.; Zhu, D. B. *Tetrahedron* **2006**, *62*, 1216–1222.
11. You, J.; Dou, L.; Yoshimura, K.; Kato, T.; Ohya, K.; Moriarty, T.; Emery, K.; Chen, C.-C.; Gao, J.; Li, G.; Yang, Y. *Nat. Commun.* **2013**, *4*, 1446.
12. Chen, J. W.; Cao, Y. *Acc. Chem. Res.* **2009**, *42*, 1709–1718.
13. Sun, X. X.; Chen, W. C.; Du, Z. K.; Bao, X. C.; Song, G. N.; Guo, K. Q.; Wang, N.; Yang, R. Q. *Polym. Chem.* **2013**, *4*, 1317–1322.
14. Liu, C.; Xiao, S. Q.; Shu, X. P.; Li, Y. J.; Xu, L.; Liu, T. F.; Yu, Y. W.; Zhang, L.; Liu, H. B.; Li, Y. L. *ACS Appl. Mater. Interfaces* **2012**, *4*, 1065–1071.
15. Liu, C.; Xu, L.; Chi, D.; Li, Y.; Liu, H.; Wang, J. *ACS Appl. Mater. Interfaces* **2012**, *5*, 1061–1069.
16. Yoshimura, K.; Matsumoto, K.; Uetani, Y.; Sakumichi, S.; Hayase, S.; Kawatsura, M.; Itoh, T. *Tetrahedron* **2012**, *68*, 3605–3610.
17. Lee, J.-K.; Fujida, K.; Tsutsui, T.; Kim, M.-R. *Sol. Energy Mater. Sol. Cells* **2007**, *91*, 892–896.
18. Lu, S. R.; Jin, T. A.; Yasuda, T.; Islam, A.; Akhtaruzzaman, M.; Han, L. Y.; Alamry, K. A.; Kosa, S. A.; Asiri, A. M.; Yamamoto, Y. *Tetrahedron* **2013**, *69*, 1302–1306.
19. Kim, K.-H.; Kang, H.; Kim, H. J.; Kim, P. S.; Yoon, S. C.; Kim, B. J. *Chem. Mater.* **2012**, *24*, 2373–2381.
20. Kim, B.; Yeom, H. R.; Choi, W. Y.; Kim, J. Y.; Yang, C. *Tetrahedron* **2012**, *68*, 6696–6700.
21. Ren, B.-Y.; Ou, C.-J.; Zhang, C.; Chang, Y.-Z.; Yi, M.-D.; Liu, J.-Q.; Xie, L.-H.; Zhang, G.-W.; Deng, X.-Y.; Li, S.-B.; Wei, W.; Huang, W. *J. Phys. Chem. C* **2012**, *116*, 8881–8887.
22. Matsuo, Y. *Chem. Lett.* **2012**, *41*, 754–759.
23. Wang, N.; Bao, X.; Yang, C.; Wang, J.; Woo, H. Y.; Lan, Z.; Chen, W.; Yang, R. *Org. Electron.* **2013**, *14*, 682–692.
24. He, Y.; Chen, H.-Y.; Hou, J.; Li, Y. *J. Am. Chem. Soc.* **2010**, *132*, 1377–1382.
25. Zhao, G.; He, Y.; Li, Y. *Adv. Mater.* **2010**, *22*, 4355–4358.
26. Matsuo, Y.; Sato, Y.; Niinomi, T.; Soga, I.; Tanaka, H.; Nakamura, E. *J. Am. Chem. Soc.* **2009**, *131*, 16048–16050.
27. Chen, S.; Ye, G.; Xiao, Z.; Ding, L. *J. Mater. Chem. A* **2013**, *1*, 5562–5566.
28. Valitov, M. I.; Romanova, I. P.; Gromchenko, A. A.; Shaikhutdinova, G. R.; Yakhvarov, D. G.; Bruevich, V. V.; Dyakov, V. A.; Sinyashin, O. G.; Paraschuk, D. Y. *Sol. Energy Mater. Sol. Cells* **2012**, *103*, 48–52.
29. Ye, G.; Chen, S.; Xiao, Z.; Zuo, Q. Q.; Wei, Q.; Ding, L. M. *J. Mater. Chem.* **2012**, *22*, 22374–22377.
30. Singh, S. P.; Kumar, C. H. P.; Nagarjuna, P.; Sharma, G. D.; Biswas, S.; Mikroyannidis, J. A. *J. Phys. Chem. C* **2013**, *117*, 13350–13356.
31. Yang, T.; Jiang, Z. Q.; Huang, X. D.; Wei, H. X.; Yuan, J. Y.; Yue, W.; Li, Y. Y.; Ma, W. L. *Org. Electron.* **2013**, *14*, 2184–2191.
32. Deng, L. L.; Xie, S. L.; Yuan, C.; Liu, R. F.; Feng, J.; Sun, L. C.; Lu, X.; Xie, S. Y.; Huang, R. B.; Zheng, L. S. *Sol. Energy Mater. Sol. Cells* **2013**, *111*, 193–199.
33. Meng, X. Y.; Xu, Q.; Zhang, W. Q.; Tan, Z. A.; Li, Y. F.; Zhang, Z. X.; Jiang, L.; Shu, C. Y.; Wang, C. R. *ACS Appl. Mater. Interfaces* **2012**, *4*, 5966–5973.
34. Choi, J. H.; Son, K. I.; Kim, T.; Kim, K.; Ohkubo, K.; Fukuzumi, S. *J. Mater. Chem.* **2010**, *20*, 475–482.
35. Hu, X.; Fu, W.; Zuo, L.; Shi, H.; Chen, M.; Liu, S.; Pan, J.; Fu, L.; Shi, M.; Chen, H. *Tetrahedron* **2013**, *69*, 3419–3424.
36. Lopez, A. M.; Mateo-Alonso, A.; Prato, M. *J. Mater. Chem.* **2011**, *21*, 1305–1318.
37. Liu, C.; Li, Y. J.; Li, C. H.; Li, W. W.; Zhou, C. J.; Liu, H. B.; Bo, Z. S.; Li, Y. L. *J. Phys. Chem. C* **2009**, *113*, 21970–21975.
38. Deng, L. L.; Feng, J.; Sun, L. C.; Wang, S.; Xie, S. L.; Xie, S. Y.; Huang, R. B.; Zheng, L. S. *Sol. Energy Mater. Sol. Cells* **2012**, *104*, 113–120.
39. Cabanetos, C.; El Labban, A.; Bartelt, J. A.; Douglas, J. D.; Mateker, W. R.; Frechet, J. M. J.; McGehee, M. D.; Beaujuge, P. M. *J. Am. Chem. Soc.* **2013**, *135*, 4656–4659.
40. Guo, X.; Cui, C. H.; Zhang, M. J.; Huo, L. J.; Huang, Y.; Hou, J. H.; Li, Y. *Energy Environ. Sci.* **2012**, *5*, 7943–7949.
41. Park, J. K.; Kim, C.; Walker, B.; Nguyen, T. Q.; Seo, J. H. *RSC Adv.* **2012**, *2*, 2232–2234.
42. Seo, J. H.; Nam, S. Y.; Lee, K. S.; Kim, T. D.; Cho, S. *Org. Electron.* **2012**, *13*, 570–578.
43. Ni, N.; Qu, B.; Tian, D.; Cong, Z. Y.; Wang, W. P.; Gao, C.; Xiao, L. X.; Chen, Z. J.; Gong, Q. H.; Wei, W. *Macromol. Chem. Phys.* **2013**, *214*, 985–993.
44. Salim, T.; Wong, L. H.; Brauer, B.; Kukreja, R.; Foo, Y. L.; Bao, Z. N.; Lam, Y. M. *J. Mater. Chem.* **2011**, *21*, 242–250.
45. Koetniyom, W.; Keawprajak, A.; Piyakulawat, P.; Jiramitmongkon, K.; Nukeaw, J.; Pratontep, S.; Asawapirom, U. *Can. J. Chem. Eng.* **2012**, *90*, 897–902.
46. Hou, J. H.; Huo, L. J.; He, C.; Yang, C. H.; Li, Y. F. *Macromolecules* **2006**, *39*, 594–603.
47. Su, M. S.; Kuo, C. Y.; Yuan, M. C.; Jeng, U. S.; Su, C. J.; Wei, K. H. *Adv. Mater.* **2011**, *23*, 3315–3319.
48. Li, Y. J.; Gan, Z. H.; Wang, N.; He, X. R.; Li, Y. L.; Wang, S.; Liu, H. B.; Araki, Y.; Ito, O.; Zhu, D. B. *Tetrahedron* **2006**, *62*, 4285–4293.
49. Jiu, T.; Li, Y.; Liu, H.; Ye, J.; Liu, X.; Jiang, L.; Yuan, M.; Li, J.; Li, C.; Wang, S.; Zhu, D. *Tetrahedron* **2007**, *63*, 3168–3172.